APPLIED AND ENVIRONMENTAL MICROBIOLOGY, Apr. 2001, p. 1718–1727 Vol. 67, No. 4
0099-2240/01/$04.00+0 DOI: 10.1128/AEM.67.4.1718–1727.2001

Characterization of Fluorescent and Nonfluorescent Peptide Siderophores Produced by *Pseudomonas syringae* Strains and Their Potential Use in Strain Identification

ALAIN BULTREYS,[1]* ISABELLE GHEYSEN,[1] HENRI MARAITE,[2] AND EDMOND DE HOFFMANN[3]

Département de Biotechnologie, Centre de Recherches Agronomiques de Gembloux, Ministère des Classes Moyennes et de l'Agriculture, B-5030 Gembloux,[1] and Unité de Phytopathologie[2] and Laboratoire de Spectrométrie de Masse,[3] Université Catholique de Louvain, B-1348 Louvain-la-Neuve, Belgium

Received 5 September 2000/Accepted 31 January 2001

Nonfluorescent highly virulent strains of *Pseudomonas syringae* pv. aptata isolated in different European countries and in Uruguay produce a nonfluorescent peptide siderophore, the production of which is iron repressed and specific to these strains. The amino acid composition of this siderophore is identical to that of the dominant fluorescent peptide siderophore produced by fluorescent *P. syringae* strains, and the molecular masses of the respective Fe(III) chelates are 1,177 and 1,175 atomic mass units. The unchelated nonfluorescent siderophore is converted into the fluorescent siderophore at pH 10, and colors and spectral characteristics of the unchelated siderophores and of the Fe(III)-chelates in acidic conditions are similar to those of dihydropyoverdins and pyoverdins, respectively. The nonfluorescent siderophore is used by fluorescent and nonfluorescent *P. syringae* strains. These results and additional mass spectrometry data strongly suggest the presence of a pyoverdin chromophore in the fluorescent siderophore and a dihydropyoverdin chromophore in the nonfluorescent siderophore, which are both ligated to a succinamide residue. When chelated, the siderophores behave differently from typical pyoverdins and dihydropyoverdins in neutral and alkaline conditions, apparently because of the ionization occurring around pH 4.5 of carboxylic acids present in β-hydroxyaspartic acid residues of the peptide chains. These differences can be detected visually by pH-dependent changes of the chelate colors and spectrophotochemically. These characteristics and the electrophoretic behavior of the unchelated and chelated siderophores offer new tools to discriminate between saprophytic fluorescent *Pseudomonas* species and fluorescent *P. syringae* and *P. viridiflava* strains and to distinguish between the two siderovars in *P. syringae* pv. aptata.

Microorganisms often live in iron-deficient environments because of the very low solubilities of the iron(III) salts near neutrality (17, 23, 24). In response to these conditions, nearly all aerobic and facultative anaerobic microorganisms that have been examined critically produce Fe(III)-chelating siderophores to provide themselves with iron (18). Consequently, the iron becomes unavailable to the microorganisms that are unable to use these siderophores, and competition for iron between microorganisms seems probable (8, 18, 34). *Pseudomonas syringae* strains belong to the fluorescent *Pseudomonas* group, which includes saprophytic, opportunistic animal pathogen and phytopathogenic species (33). Strains belonging to this group most generally produce siderophores that fluoresce under UV light. Phytopathogenic *P. syringae* strains are very efficient and ubiquitous colonists of plant surfaces (15, 21). A better understanding of the ecological benefits of these pathogens is necessary if efficient methods of biological control are to be developed. Recently, it was shown that an apparently identical fluorescent peptide siderophore is produced by strains belonging to distantly related pathovars of *P. syringae* and to the closely related phytopathogenic species *Pseudomonas viridiflava* (7). The spectral characteristics of the molecule differ from those of typical pyoverdins (7), which are the fluorescent peptide siderophores generally produced by saprophytic and opportunistic animal pathogen fluorescent *Pseudomonas* species (2, 4). The production of the fluorescent siderophore by *P. syringae* is activated under conditions that are related to conditions encountered on plant surfaces (7, 23, 30, 42, 43). Therefore, as the siderophore has a rather high Fe(III)-binding constant of about 10^{25} (9) and has specificity for *P. syringae* strains (7), it seems probable that this siderophore plays a role in the interactions between microorganisms on plants (7, 9, 10). Therefore, it could represent one of the ecological benefits of *P. syringae* strains.

The existence of nonfluorescent *P. syringae* strains (33), however, raises some questions. Although some of these strains were shown to be able to use the fluorescent peptide siderophore generally produced in the species (7), the way such strains adapt to iron-limiting conditions in the absence of other *P. syringae* strains remains unclear. Furthermore, these strains are not ecologically disadvantaged since they include highly virulent and widespread strains of *P. syringae* pv. morsprunorum (6, 7, 13) and of *P. syringae* pv. aptata (26). Two explanations could be that these strains may need particular conditions to produce the fluorescent siderophore or that they may produce different siderophores.

The fluorescence of unchelated pyoverdins results from the presence of the quinoline chromophore (Fig. 1A), which is bound to a peptide chain and to a dicarboxylic acid or a

* Corresponding author. Mailing address: Département de Biotechnologie, Centre de Recherches Agronomiques de Gembloux, 234 Chaussée de Charleroi, B-5030 Gembloux, Belgium. Phone: (32) 81 62 73 88. Fax: (32) 81 62 73 99. E-mail: bultreys@cragx.fgov.be.

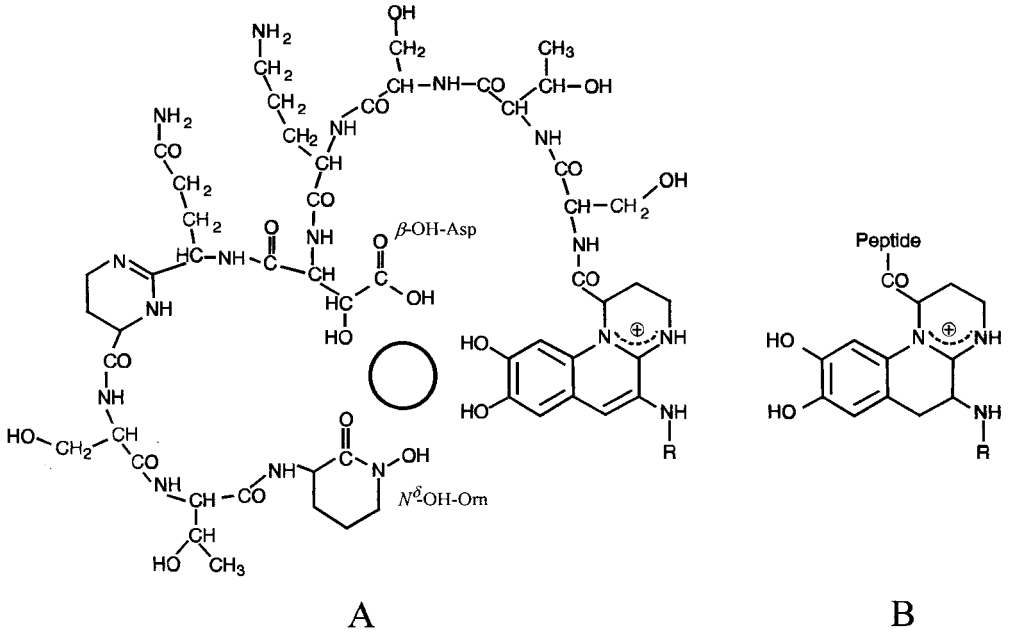

FIG. 1. Example of a pyoverdin (A) and the cognate dihydropyoverdin (B) produced by a *P. putida* strain (16). The circle in the center of the molecule (A) indicates the place where the iron is chelated to three bidentate iron-binding ligands; one of the bidentate ligands of the peptide chain is β-OH-Asp, and the second is N^{δ}-OH-Orn. Iron chelation involves the loss of one hydrogen from each of the three iron-binding ligands. Siderophores with different radical (R) side chains are detected in culture. The peptide chains vary among strains and species.

dicarboxylic amide, but the Fe(III)-chelated pyoverdins do not fluoresce (2). Each pyoverdin is based on a common theme of three iron-binding ligands, one of which is always an *o*-dihydroxy aromatic group derived from quinoline located in the chromophore. The other two are located in the peptide chain and are hydroxamic acids derived from ornithine, either acylated N^{δ}-hydroxyornithine (N^{δ}-acyl-N^{δ}-OH-Orn) or cyclized N^{δ}-hydroxyornithine (N^{δ}-OH-Orn), or one hydroxamic acid derived from ornithine plus a β-hydroxyaspartic acid (β-OH-Asp) residue (Fig. 1A) (2, 4). The spectral characteristics in the visible and the color of Fe(III)-chelated pyoverdins depend on the chromophore (2). Although the iron-binding sites of both the quinoline chromophore and the β-OH-Asp residues contain two hydroxy groups (Fig. 1A), iron chelation involves the loss of one hydrogen from only one hydroxy group in each of the three iron-binding ligands. Numerous pyoverdin structures have now been published for saprophytic and opportunistic animal pathogen fluorescent *Pseudomonas* species, but only one has been reported for phytopathogenic fluorescent *Pseudomonas* species (4). Evidence of the presence of the pyoverdin chromophore was obtained by the observation of typical spectral characteristics, by comparing nuclear magnetic resonance data with the published data for the first characterized pyoverdin (38), whose structure was determined by crystal X-ray diffraction methods (39), and by the detection of a characteristic retro-Diels-Alder (RDA) fragment ion in fast atom bombardment (FAB) mass spectrometry analyses (1, 2, 29). Dihydropyoverdins differ from pyoverdins only with respect to the saturation of two carbon atoms of the chromophore (Fig. 1B); consequently, the unchelated molecules do not fluoresce (16, 37, 38). These molecules are putative precursors of pyoverdins (3, 4) that were sometimes found in association with the cognate pyoverdin (16, 35, 37, 38).

In this report we show that highly pathogenic nonfluorescent strains of *P. syringae* pv. aptata isolated from sugar beet in different European countries and in Uruguay (26) produce a nonfluorescent peptide siderophore. The molecule has been purified and characterized. Comparison with the fluorescent peptide siderophore generally produced in the species (7, 9) revealed that the molecules are closely related. The results suggest close similarities between these molecules and pyoverdins and dihydropyoverdins. Detection tests indicate that nonfluorescent *P. syringae* strains belonging to pathovars other than pathovar aptata do not produce the nonfluorescent peptide siderophore. It appears that these peptide siderophores are of potential interest in strain classification and identification.

MATERIALS AND METHODS

Bacterial strains and culture conditions. The characteristics of the strains used in this study are described in Table 1. *P. syringae* pv. aptata strains include well-characterized (26) fluorescent and nonfluorescent European and Uruguayan isolates; unlike the fluorescent strains, the nonfluorescent strains are unable to use myoinositol (26). All precultures were grown at 28°C on medium 2 agar (6); liquid cultures were grown unshaken at 20°C in petri dishes containing 10 ml of GASN liquid medium and one block of GASN agar medium (7). The production of fluorescent pigments was investigated on King's medium B (19) and on GASN agar.

Detection, production, and purification of a nonfluorescent siderophore. Liquid cultures of nonfluorescent strains of *P. syringae* pv. aptata and *P. syringae* pv. morsprunorum were started in GASN medium (7) and incubated for about 72 h at 20°C. After the addition of 40 μl of an $FeCl_3$ solution (1 M), the liquid fractions were stirred for 20 min, centrifuged (22 min, 10,000 × *g*), and filtered through a 0.2-μm-pore-size membrane filter. Unusual color changes resulting

TABLE 1. Characteristics of strains used in this study

Strain[a]	RFLP cluster[b]	Host or origin	Country	Fluorescence on medium[c]		Siderophores detected in GASN medium[d]	Molecular mass of dominant siderophore (amu)[e]	Source or reference
				King's B	GASN agar			
P. syringae pv. aptata	S2B							
LMG 5059^T		Sugar beet	United States	+	+	Pa	1,175	LMG[f]
LMG 5143		Sugar beet	Unknown	+	+	Pa		LMG
LMG 5646		Sugar beet	New Zealand	+	+	Pa		LMG
UPB 152		Sugar beet	Switzerland	+	+	Pa		26
UPB 156		Sugar beet	Italy	+	+	Pa		26
UPB 225		Sugar beet	Germany	+	+	Pa		26
UPB 339		Sugar beet	Sweden	+	+	Pa		26
UPB 110		Sugar beet	Belgium	−	−	DPa	1,177	26
UPB 133		Sugar beet	The Netherlands	−	−	DPa	1,177	26
UPB 165		Sugar beet	France	−	−	DPa	1,177	26
UPB 221		Sugar beet	Uruguay	−	−	DPa	1,177	26
P. syringae pv. syringae	S2B							
LMG 1247^T		Lilac	England	+	+	Pa	1,175	LMG
B301D		Pear	England	+	+	Pa	1,175	6
PsP2		Pear	Belgium	+	+	Pa	1,175	6
P. syringae pv. garcae LMG 5064^T	S2B	Coffee	Brazil	−	−	—		LMG
P. syringae pv. morsprunorum	S2A							
LMG 5075 t_1^T		Plum	Unknown	+	+	Pa	1,175	LMG
LMG 2222		Sweet cherry	England	+	+	Pa	1,175	LMG
PmC14		Sweet cherry	Belgium	+	+	Pa	1,175	6
PmC28		Sweet cherry	Belgium	−	−	—		This study
PmC36		Sweet cherry	Belgium	−	−	—		6
PmC46		Sweet cherry	Belgium	−	−	—		This study
PmC53		Sweet cherry	Belgium	−	−	—		This study
P. syringae pv. tomato LMG 5093^T	S1	Tomato	England	+	+	Pa	1,175	LMG
P. syringae pv. apii LMG 2132^T	S1	Celery	United States	+	−	—		LMG
P. syringae pv. lachrymans LMG 5070^T	S1	Cucumber	United States	±	±	Pa		LMG
P. syringae pv. persicae LMG 5184^T	S1	Peach	France	−	−	—		LMG
P. syringae pv. cannabina LMG 5096^T	ND	*Cannabis sativa*	Hungary	−	−	—		LMG
P. syringae pv. sesami LMG 2289^T	ND	Sesame	Yugoslavia	−	−	—		LMG
P. viridiflava LMG 2352^T	V	Bean	Switzerland	+	+	Pa	1,175	LMG
P. fluorescens strains								
LMG 1244		Polluted seawater	Denmark	+	+	Pt		LMG
LMG 1794^T		Water	Englang	+	+	Pt	1,212	LMG
LMG 5822		Creamery waste	Unknown	v	NT	NT		LMG
LMG 5916		Tap water	Unknown	+	+	Pt		LMG
LMG 14674		Hen's egg	Unknown	+	+	Pt		LMG
P. chlororaphis LMG 5004^T		Contaminated plate	Unknown	+	+	Pt		LMG
P. putida								
LMG 1246		Unknown	Unknown	+	+	Pt		LMG
LMG 2257^T		Soil	United States	+	+	Pt		LMG
LMG 5835		Soil	Unknown	+	+	Pt		LMG

[a] Superscript "T" denotes pathotype or type strain.
[b] Data from reference 25. S1, first cluster of *P. syringae*; S2A, first subcluster in the second cluster of *P. syringae*; S2B, second subcluster in the second cluster of *P. syringae*; ND, position not determined; V, *P. viridiflava* cluster.
[c] Data from this study. +, positive; −, negative; +/−, weak production; v, variable results; NT, not tested.
[d] Data from this study. Detection was made by observation of pH-dependent color changes, by spectrophotometry, or by IEF. Pa, atypical pyoverdins; DPa, atypical dihydropyoverdins; Pt, typical pyoverdins; —, no siderophore detected; NT, not tested.
[e] Molecular mass of the Fe(III)-chelated pyoverdin measured by ESI mass spectrometry after total purification of the molecules (data from this study).
[f] LMG, Laboratorium voor Microbiologie van Gent, Belgian Coordinated Collections of Microorganisms, Ghent, Belgium.

from the addition of $FeCl_3$ indicated the probable chelation of a siderophore. The pigments were produced and purified as previously described (7) except that detection and purity assessments were performed at 310 and 530 nm rather than at 403 nm. The presence of iron in the pigment purified from $FeCl_3$-supplied GASN culture supernatants of strain UPB 221 was investigated by decomplexation experiments using EDTA (9) and 8-hydroxyquinoline (27) as strong iron chelators.

Regulation of the production of the nonfluorescent siderophore by iron. The repression of siderophore production by iron was investigated by increasing the Fe(III) concentration of GASN medium by 0, 1, 5, 10, and 20 μM following the addition of increasing quantities of EDTA-iron(III) sodium salt [Fe(III)-EDTA]. Iron was autoclaved separately and supplied after autoclaving. Iron-free glassware (32), high-purity glucose and asparagine (Sigmaultra; Sigma), and 10 g of SeaPlaque agarose (FMC) per liter of culture medium were used to ensure ultralow levels of contaminating iron. Five cultures of *P. syringae* pv. aptata UPB 133 per treatment were analyzed after 3 days of growth at 20°C. Bacterial growth was estimated by measuring the absorbance at 650 nm on culture medium diluted three times with water. Then, 36 μl of a $FeCl_3$ solution (1 M) was added to the volume (approximately 9 ml) collected from each petri dish culture. Each solution was then stirred for 20 min, centrifuged (12 min, 10,000 × *g*), and filtered. The pH of each solution was adjusted to 7.0, and siderophore production was estimated by measuring the absorbance at 490 nm. The experiments were replicated.

Amino acid and mass spectrometry analyses. The amino acid composition of siderophores produced by strains UPB 110 and UPB 165 was determined as previously described (7). Molecular masses of the purified molecules were determined by electrospray ionization (ESI) with an Ion Trap Finnigan MAT LCQ mass spectrometer used in the direct infusion mode. The similarity of the molecules was ascertained by comparing the tandem mass (MS/MS) spectra of the molecular ions. Analyses were carried out for the purified Fe(III)-chelated siderophores produced by the nonfluorescent strains UPB 110, UPB 133, UPB 165, and UPB 221 of *P. syringae* pv. aptata; by the closely related fluorescent strains *P. syringae* pv. aptata LMG 5059 and *P. syringae* pv. syringae LMG 1247, PsP2 and B301D; by the fluorescent more distantly related strains *P. syringae* pv. tomato LMG 5093 and *P. syringae* pv. morsprunorum LMG 5075 t1, LMG 2222, and PmC14; by *P. viridiflava* LMG 2352; and by *P. fluorescens* LMG 1794 (Table 1). The 10 latter molecules had been purified in a previous study (7). Mass spectrometry analyses were carried out for the unchelated siderophores produced by the strains *P. syringae* pv. tomato LMG 5093 and *P. syringae* pv. aptata UPB 110. FAB mass spectrometry analyses were also carried out for the unchelated siderophore of *P. syringae* pv. tomato LMG 5093 with a Finnigan MAT TSQ 700 mass spectrometer, using thioglycerol as a matrix, in order to detect a fragment ion resulting from the RDA decomposition of the pyoverdin chromophore (29, 41). This RDA fragment results from the loss of the quinoline part of the chromophore, together with the acid side chain; it is diagnostic of the pyoverdin chromophore and of its acid side chain (1, 11, 16, 22, 29, 41).

Spectral analyses. Fe(III)-chelated siderophore of *P. syringae* pv. morsprunorum LMG 2222 purified in a previous study (7) was decomplexed in a solution of EDTA (1 M) in a 30 mM NaOH-formic acid buffer at pH 5.0. The unchelated molecule was subsequently purified on an octadecylsilane column. The spectral characteristics of this molecule and of Fe(III)-chelated siderophores of *P. syringae* pv. syringae B301D and *P. syringae* pv. aptata UPB 133 were determined at pH 3.0, 3.5, and 4.0 in 100 mM NaOH-formic acid buffers; at pH 4.5, 5.0, and 5.5 in 100 mM NaOH-acetic acid buffers; and at pH 6.0 and 7.0 in 100 mM NaOH-phosphoric acid buffers. Analyses were carried out using a model UV-2101PC UV-visible light spectrophotometer (Shimadzu). Analyses were also carried out with a purified Fe(III)-chelated pyoverdin produced by *P. fluorescens* LMG 1794, whose spectral characteristics at pH 7.0 correspond to those of chelated typical pyoverdins (2, 7, 11). The unchelated siderophore of *P. syringae* pv. aptata UPB 133 was obtained by treating a concentrated solution of purified Fe(III)-chelated siderophore with 3 volumes of 20% 8-hydroxyquinoline in chloroform. The aqueous solution was washed with chloroform and evaporated. The siderophores were rechromatographed on a DEAE-Sephadex column eluted first isocratically and then with a gradient 0.05 to 1 M NaOH-acetic acid (pH 5.0). The unchelated molecule was collected, and its spectral characteristics were determined at pH 5.0. After desalting and evaporation, the molecule was redissolved in a 100 mM NaOH-phosphoric acid buffer, and its spectral characteristics were determined at pH 7.0.

Transformation of the nonfluorescent peptide siderophore into the cognate fluorescent molecule. A diluted solution of purified unchelated siderophore of *P. syringae* pv. aptata UPB 133 in a NaOH-acetic acid buffer at pH 5.0 was obtained as described above and divided in two fractions. The pH of the first fraction was increased to pH 10 with NaOH and then directly reduced to pH 5.0 with HCl. Aliquots (60 μl) of both solutions were loaded on a horizontal isoelectric focusing (IEF) gel (Ampholine PAG plate, pH 3.5 to 9.5; Pharmacia) at 4°C (20, 28). The gel was run at constant power (12 W) until the voltage reached 1,000 V, and it was observed under UV light (wavelength, 360 nm). A similar fraction maintained for 5 min at pH 10 was subsequently desalted on an octadecylsilane column and evaporated. It was redissolved in 20 ml of a 10 mM NaOH-phosphoric acid buffer (pH 7.0), complexed by the addition of 80 μl of a $FeCl_3$ solution (1 M), desalted, and evaporated. A fraction showing chromatographic characteristics similar to the Fe(III)-chelated dominant fluorescent and nonfluorescent siderophores of *P. syringae* was collected after separation on a CM C25 Sephadex column (7) and analyzed by mass spectrometry.

Determination of the Fe(III)-binding constant of the nonfluorescent siderophore. The apparent stability constant at pH 7.0 of the peptide siderophore produced by the nonfluorescent strain *P. syringae* pv. aptata UPB 133 was determined by using EDTA as a competitive chelator as described by Meyer and Abdallah (27). Solutions containing 160 μM Fe(III)-chelate and 15 mM EDTA were prepared in a 100 mM phosphate buffer (pH 7.0). Known amounts of the solutions of EDTA and Fe(III)-chelated siderophore were added to a 160 μM solution of Fe(III)-chelated siderophore in the same buffer to obtain a final volume of 6 ml. Absorbances were analyzed at 550 nm until constant values were reached.

Growth stimulation tests. Growth stimulation tests were carried out as previously described (7) except that dipyridyl was generally used instead of ethylenediaminedihydroxyphenylacetic acid as a strong iron chelator. Dipyridyl was tested at 0.11 and at 0.16 g per liter in King's medium B agar; the plates were incubated at 28°C and observed during the following 24 and 48 h, respectively.

Visual and spectrophotochemical detection of siderophore production. Each strain was grown for 3 days in one petri dish containing 10 ml of GASN liquid medium and one block of GASN agar medium (7). Then 36 μl of an $FeCl_3$ solution (1 M) was added, and the cultures were shaken for 20 min, centrifuged (20 min, 10,000 × *g*), and filtered. The pH was modified between pH 3.0 and 7.0, and the colors of the solutions were noted. After being possibly diluted three times, when the siderophores were too concentrated to be directly analyzed, the culture media equilibrated at pH 7.0 were analyzed with a model Lambda 5 UV-VIS spectrophotometer (Perkin-Elmer), starting from 700 to 360 nm. Liquid GASN medium was used as a control. Among the strains analyzed were the strains listed in Table 1 and unidentified oxidase-positive fluorescent strains isolated from the field.

Siderophore detection by IEF and CAS overlay. The technique described by Koedaen et al. (20) and modified by Meyer et al. (28) was used. It combines the separation of the peptide siderophores by IEF and their detection, either under UV light (wavelength, 360 nm) or by overlaying the IEF gel with an agarose gel containing a hexadecyltrimethylammonium bromide-Fe(III)-chrome azurol S (CAS) blue complex; in the presence of a siderophore, the agarose gel color locally changes to orange following decomplexation of the blue complex (36). Filtered culture supernatants (40 μl) of GASN cultures in petri dishes containing agar blocks were directly loaded on sample application pieces. The technique was used to screen nonfluorescent or weakly fluorescent strains of *P. syringae* (Table 1) for the production of the nonfluorescent peptide siderophore. The technique was modified to be carried out with Fe(III)-chelated siderophores. Forty microliters of an $FeCl_3$ solution (1 M) was added to 10 ml of GASN culture supernatants. After filtration, aliquots (60 μl) were loaded on the IEF gel. The violet or brown bands were visually detected.

RESULTS

Detection, production, and purification of a nonfluorescent siderophore. When iron was added to nonfluorescent cultures of nonfluorescent strains of *P. syringae* pv. aptata, the color of the GASN culture media abruptly changed from pale yellow to greyish violet. After filtration, the culture media were bluish violet at acidic pH values and pinkish mauve at neutral pH values. These reactions were not observed with nonfluorescent strains of *P. syringae* pv. morsprunorum. In preliminary experiments, the unknown colored molecules behaved similarly to the Fe(III) chelate obtained from the fluorescent siderophore produced by fluorescent *P. syringae* strains. Therefore, the same procedures were adopted to produce and purify, after addition of $FeCl_3$, the dominant pigments detected in cultures of strains UPB 110, UPB 133, UPB 165, and UPB 221 of *P.*

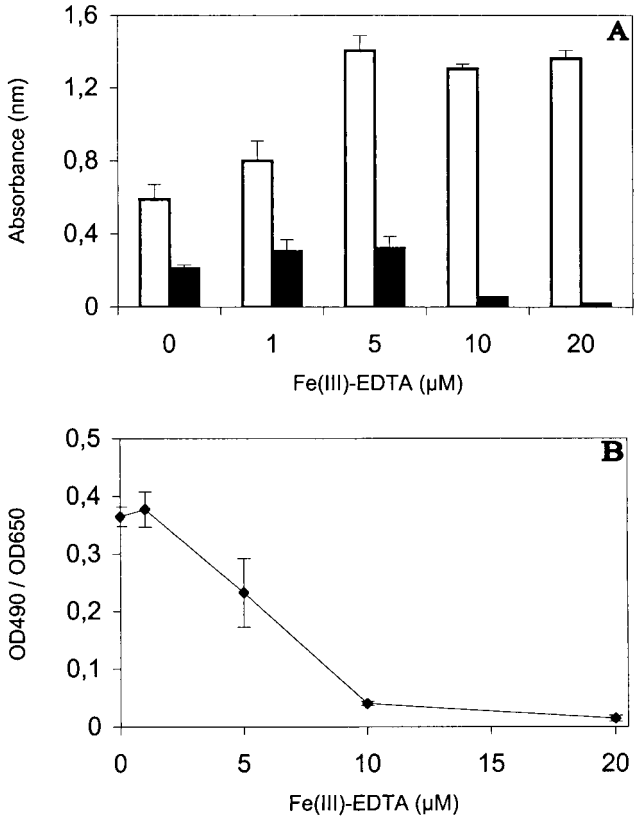

FIG. 2. Influence of Fe(III)-EDTA on *P. syringae* pv. aptata UPB 133 grown for three days in GASN medium and estimation of siderophore production. Columns represent means ± standard deviations for absorbance at 650 nm (□) and 490 nm (■) (A), and the curve shows the ratio of these absorbances (B). Absorbance (optical density) was measured at 650 nm (OD650) by using thrice-diluted cultures and, after bacteria were eliminated, at 490 nm (OD490) by using undiluted cultures.

syringae pv. aptata. An amount of about 30 mg of purified pigment per liter of culture medium was usual. The presence of iron in the molecule was confirmed by the decomplexation experiments, which resulted in total discoloration of the solutions of siderophore.

Regulation of the production of the nonfluorescent siderophore by iron. The highest siderophore production estimated on basis of the absorbance at 490 nm occurred when 5 μM Fe(III)-EDTA was added to GASN medium (Fig. 2A), but the culture media were iron deficient at the two lowest concentrations of Fe(III)-EDTA tested. Figure 2B shows that the actual activation of siderophore production was best at the two lowest concentration of Fe(III)-EDTA tested. It was already partially repressed when 5 μM Fe(III)-EDTA was added to GASN medium, and it was almost completely repressed by the addition of 10 and 20 μM Fe(III)-EDTA.

Amino acid and mass spectrometry analyses of nonfluorescent and fluorescent siderophores produced by *P. syringae*. The siderophores produced by the nonfluorescent strains UPB 110 and UPB 165 of *P. syringae* pv. aptata contained two hydroxyaspartic acid, two serine, and two threonine residues and one lysine residue. The observed composition corresponded to the known amino acid composition of the fluorescent siderophore generally produced in the species (7, 9).

The Fe(III) chelates obtained from the nonfluorescent siderophores produced by the nonfluorescent strains of *P. syringae* pv. aptata had a molecular mass measured by ESI of 1,177 atomic mass units (amu), and the Fe(III) chelates obtained from the fluorescent siderophores produced by the fluorescent strains of *P. syringae* and *P. viridiflava* had a measured molecular mass of 1,175 amu. The total identity of the molecules was confirmed in each group of strains by comparing the MS/MS spectra of the molecular ions. The unchelated molecules had molecular masses of 1,124 and 1,122 amu. As expected, this corresponds to a difference of 53 amu in comparison with values for the respective Fe(III) chelates [-1 (^{56}Fe)$+3$ (^{1}H)]. A difference of two mass units was consistently found between the fluorescent and nonfluorescent siderophores, and the essential fragment ions observed in the source spectra or in the MS/MS spectra of both molecules were either identical or two mass units higher in the spectra of the nonfluorescent siderophore. An RDA fragment ion of *m/z* 819 was observed in the negative-ion FAB spectra of the fluorescent siderophore. This ion resulted from a loss of 302 mass units from the molecular ion of *m/z* 1121 and revealed the likely presence of a pyoverdin chromophore ligated to a succinamide residue.

Spectral analyses of the fluorescent peptide siderophore. The spectral characteristics of the unchelated fluorescent siderophore produced by *P. syringae* pv. morsprunorum LMG 2222 were similar to those reported for typical pyoverdins (2, 27), with maxima in the visible observed at about 378 and 365 nm at pH ≤5.0 and at about 402 nm at pH 7.0. However, when chelated to the iron (Fig. 3A and 4A), the molecule behaved differently from the Fe(III)-chelated typical pyoverdin of *P. fluorescens* LMG 1794, which had expected pH-independent spectral characteristics between pH 7.0 and 3.0. The maximum observed near 408 nm at pH 7.0 and 6.0 shifted to 406 nm at pH 5.0 and to 402.5 nm at pH 4.0 (Fig. 4A), and the color of the molecule changed from orange-yellow to a darker orange-beige color. From pH 4.0, one broad charge transfer band similar to that observed for the Fe(III)-chelated typical pyoverdin was observed at about 550 nm (Fig. 4A). Between pH 4.0 and 3.0, the molecule became brown-beige and gradually acquired all of the spectral characteristics of the Fe(III)-chelated typical pyoverdin: a maximum in the visible near 399 nm with a log ε of 4.19 and two broad charge transfer bands at about 470 and 550 nm (Fig. 3A). The changes between pH 3.0 and 5.5 were reversible.

Spectral analyses of the nonfluorescent peptide siderophore. The unchelated nonfluorescent siderophore produced by *P. syringae* pv. aptata UPB 133 was colorless and had no maximum in the visible. One maximum at about 297 nm similar to that reported for unchelated dihydropyoverdins (16) was observed at pH 5.0 and 7.0. The absorbance totally disappeared near 400 nm at pH 5.0 and almost totally at pH 7.0; total disappearance was observed near 575 nm at pH 7.0. The Fe(III)-chelated molecule was pinkish mauve at pH 7.0 and 6.0, and it showed maxima near 242, 311, and 490 nm (Fig. 3B and 4B). The maxima near 242 and 311 nm were nearly pH independent (Fig. 4B). The maximum at 490 nm moved to 517 nm at pH 5.0, 553 nm at pH 4.5, and 563 nm at pH 4.0 (Fig. 4B). From pH 4.5, the molecule was bluish violet and had

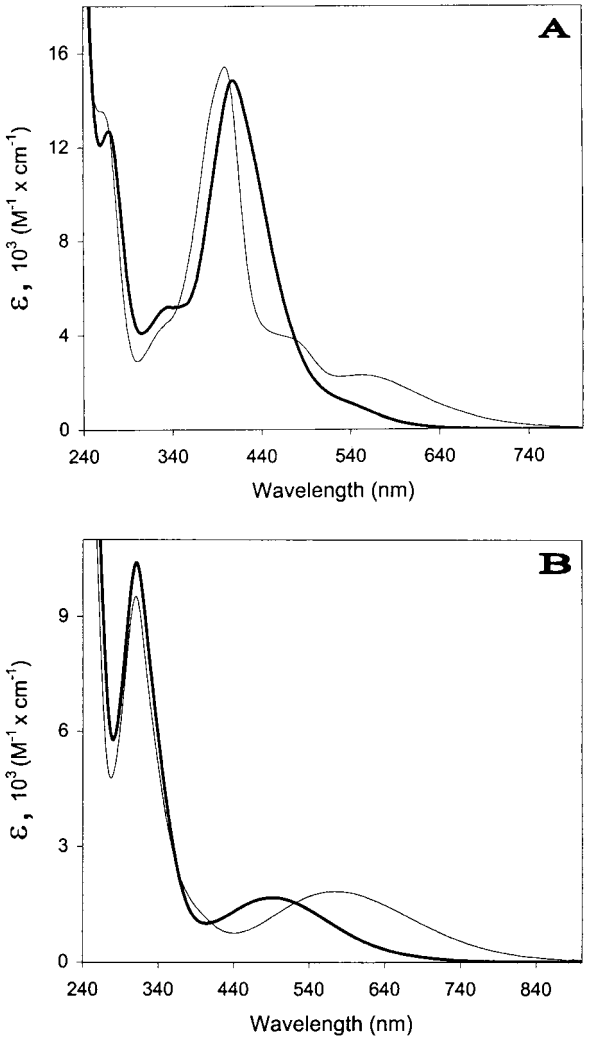

FIG. 3. Differences between the absorption spectra of the Fe(III)-chelated siderophore of *P. syringae* pv. syringae B301D (A), and *P. syringae* pv. aptata UPB 133 (B) in 100 mM phosphate buffer at pH 7.0 (dark line) and in 100 mM formate buffer at pH 3.0 (light line).

spectral characteristics resembling those reported for Fe(III)-chelated dihydropyoverdins (16, 37). The maximum in the visible was observed near 572 nm at pH 3.5 and 3.0 (Fig. 3B).

Detection of isosbestic points between spectra. The absorption spectra of the Fe(III)-chelated fluorescent and nonfluorescent siderophores were similarly influenced by the pH between 5.5 and 3.5 (Fig. 4): isosbestic points were observed between spectra, indicating that a unique modification occurred for each molecule. However, a weak displacement was detectable at pH 4.0 and 3.5 in Fig. 4B for the isosbestic point located near 520 nm; this suggested that other changes probably occurred in the case of the Fe(III)-chelated nonfluorescent siderophore, possibly in relation to the behavior of Fe(III)-chelated dihydropyoverdins which have pH-dependent spectral characteristics (2).

Transformation of the nonfluorescent siderophore in the cognate fluorescent molecule. Fluorescence was detectable at pH 5.0 in an initially nonfluorescent solution of purified unchelated nonfluorescent siderophore when the pH of this solution was transiently increased to 10.0. Comparison of the IEF patterns obtained from the initial and the modified solutions (Fig. 5) confirmed appearances of fluorescent molecules apparently corresponding to fluorescent siderophores produced by strain *P. syringae* pv. aptata LMG 5059. Several bands were observed, indicating that the molecules were unstable at pH 10.0. After chelation to the iron, ESI-mass spectrometry enabled the detection of molecules with molecular masses of 1,175 and 1,177 amu, and MS/MS spectra confirmed the presence of the Fe(III) chelate of the fluorescent siderophore. This proved the transformation of the nonfluorescent siderophore in the cognate fluorescent one.

Determination of the Fe(III)-binding constant of the nonfluorescent siderophore. Absorbance was measured at 550 nm because spectral analyses at pH 7.0 indicated that absorbance of the unchelated siderophore was negligible at this wavelength. The mean value calculated for the Fe(III)-binding constant of the nonfluorescent siderophore at pH 7.0 was 1.9

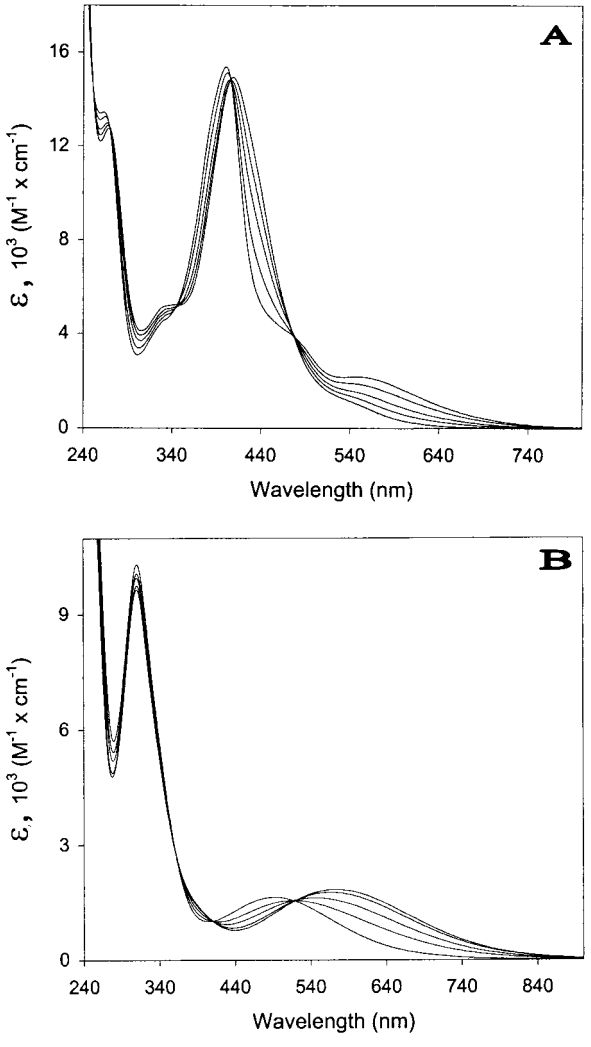

FIG. 4. Absorption spectra of the Fe(III)-chelated siderophores of *P. syringae* pv. syringae B301D (A) and *P. syringae* pv. aptata UPB 133 (B) at pH 6.0 (lower ε at 640 nm), 5.0, 4.5, 4.0, and 3.5 (higher ε at 640 nm).

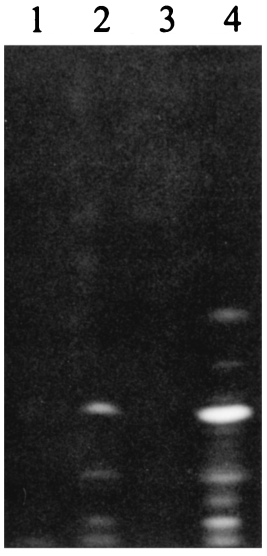

FIG. 5. IEF patterns obtained under UV light (wavelength, 360 nm) from acetate buffer solutions of siderophores and from filtered GASN culture supernatants. Lanes 1 and 4, supernatants (40 μl) of 3-day GASN cultures of the nonfluorescent strain *P. syringae* pv. aptata UPB 221 (lane 1) and the fluorescent strain *P. syringae* pv. aptata LMG 5059 (lane 4); lanes 2 and 3, solutions (60 μl) of purified nonfluorescent siderophore of *P. syringae* pv. aptata UPB 133 in acetate buffer (pH 5.0) transiently increased to pH 10.0 (lane 2) or not (lane 3).

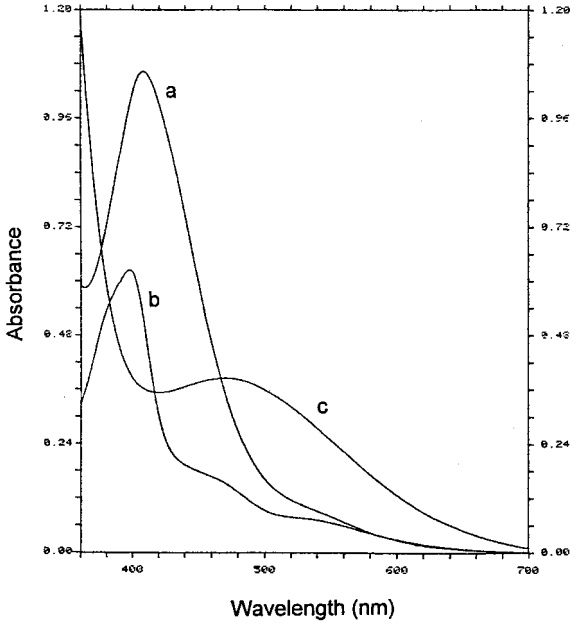

FIG. 6. Absorption spectra of filtered thrice-diluted supernatants of 3-day GASN cultures of *P. syringae* pv. syringae LMG 1247 (curve a) and *P. putida* LMG 2257 (curve b), as well as of filtered undiluted supernatant of a 3-day GASN culture of *P. syringae* pv. aptata UPB 133 (curve c), containing Fe(III)-chelated siderophores.

(± 0.25) $\times$ 10^{24}, which was lower than that of the cognate fluorescent siderophore (9).

Growth stimulation tests. The growth on iron-deficient media of the four nonfluorescent strains of *P. syringae* pv. aptata tested (UPB 110, UPB 133, UPB 165, and UPB 221) and the three fluorescent strains of *P. syringae* tested (LMG 5059, PsP2, and LMG 5093) was stimulated by the Fe(III)-chelated siderophore of strain *P. syringae* pv. aptata UPB 133. Also, the nonfluorescent strain *P. syringae* pv. morsprunorum PmC36, but not *P. fluorescens* LMG 5822, could use this siderophore.

Visual and spectrophotochemical detection of siderophore production. The visual detection of Fe(III)-chelated siderophores in GASN medium proved to be reliable for differentiating saprophytic fluorescent *Pseudomonas* strains from fluorescent strains of *P. syringae* and from nonfluorescent strains of *P. syringae* pv. aptata. This could be done by detecting the darkening of the color of the culture medium between pH 5.3 and 4.0. Solutions of Fe(III)-chelated pyoverdins produced by saprophytic fluorescent *Pseudomonas* strains were red-brown to orange-beige, depending on the concentration, in these conditions. However, the color of the solutions changed abruptly from brown-beige (near pH 3.0) or orange-beige (near pH 4.3) to orange or orange-yellow, depending on the concentration, above pH 5.3 for the fluorescent strains of *P. syringae*, and from bluish violet (below pH 4.3) to pinkish mauve (above pH 5.3) for the nonfluorescent strains of *P. syringae* pv. aptata. The colors of the solutions were generally different enough at pH 7.0 to draw conclusions as to the classification of a strain. The results were always confirmed by the detection of the expected spectral characteristics at pH 7.0 (Fig. 6). However, the maxima in the visible were observed near 470 nm for the cultures of nonfluorescent strains of *P. syringae* pv. aptata (Fig. 6) rather than near 490 nm for the purified dominant Fe(III) chelate (Fig. 3B). None of the two techniques enabled siderophore detection for the nonfluorescent strains of other *P. syringae* pathovars investigated (Table 1).

Siderophore detection by IEF and CAS overlay. An example of an IEF analysis including fluorescent and nonfluorescent *P. syringae* strains is shown in Fig. 7. Observations of IEF gels under UV light enabled the detection of one characteristic dominant band and several secondary bands for every fluorescent strain of *P. syringae* investigated, but no fluorescent bands were detected in the patterns of nonfluorescent strains of *P.*

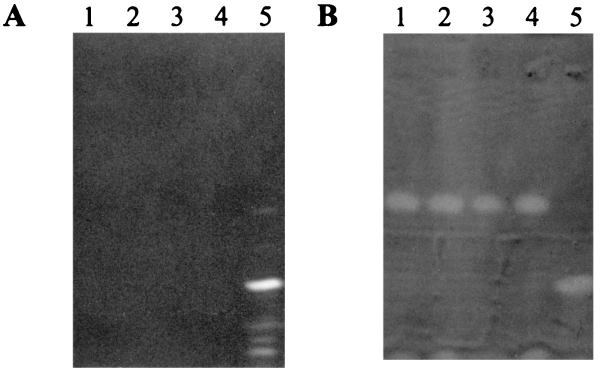

FIG. 7. IEF patterns obtained from filtered 3-day GASN culture supernatants (40 μl) observed under UV light (wavelength, 360 nm) (A) and after CAS overlay (B). Lane 1, *P. syringae* pv. aptata UPB 133; lane 2, *P. syringae* pv. aptata UPB 110; lane 3, *P. syringae* pv. aptata UPB 165; lane 4, *P. syringae* pv. aptata UPB 221; lane 5, *P. syringae* pv. aptata LMG 5059.

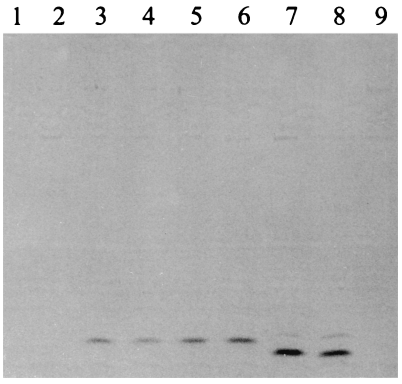

FIG. 8. IEF patterns obtained from filtered 3-day GASN culture supernatants (60 μl) containing Fe(III)-chelated siderophores. Lane 1, uninoculated GASN medium; lane 2, *P. syringae* pv. morsprunorum PmC36; lane 3, *P. syringae* pv. aptata UPB 221; lane 4, *P. syringae* pv. aptata UPB 110; lane 5, *P. syringae* pv. aptata UPB 133; lane 6, *P. syringae* pv. aptata UPB 165; lane 7, *P. syringae* pv. morsprunorum LMG 2222; lane 8, *P. syringae* pv. aptata LMG 5059; lane 9, *P. fluorescens* LMG 1794. The bands are violet in lanes 3 to 6 and brown in lanes 7 and 8.

syringae pv. aptata (Fig. 7A). Secondary bands appeared to be more important when the final pH of the culture medium was high, and they resulted from the known (27) increasing concentrations of transformation products associated with high pH values (unpublished results). The pattern of fluorescent *P. syringae* strains was easily differentiated from those of saprophytic fluorescent *Pseudomonas* strains (not shown). However, one characteristic dominant band and a second band located near the anode were detected following CAS overlay in the patterns of all nonfluorescent strains of *P. syringae* pv. aptata investigated (Fig. 7B). The dominant band was never detected in the patterns of fluorescent strains of *P. syringae*. The results confirmed that the fluorescent strains apparently do not produce the nonfluorescent molecule, or do so in a way not detectable in the tests described here, and conversely. Some weak fluorescence, however, was sometimes observed in cultures of nonfluorescent strains of *P. syringae* pv. aptata when the final pH of the culture medium exceeded 7.0, but this could have resulted from the observed natural base-catalyzed conversion of the nonfluorescent molecule into fluorescent molecules (Fig. 5). All other nonfluorescent strains of *P. syringae* tested gave no bands in the IEF analyses with both methods of detection. The weakly fluorescent strain on GASN agar medium *P. syringae* pv. lachrymans LMG 5070 (Table 1) gave poorly detectable fluorescent bands, but the nonfluorescent siderophore was not detected. IEF analyses performed with Fe(III)-chelated siderophores allowed the simple and simultaneous visual detection of the chelates (Fig. 8). However, the technique was not adaptable for all pyoverdins, since the isoelectric points of the Fe(III)-chelated pyoverdins produced by *P. fluorescens* LMG 1794 were too high to be analyzed in this way (Fig. 8, lane 9).

DISCUSSION

As microorganisms most generally produce siderophores in response to iron-limiting conditions (18), we investigated the production of siderophores by strains of *P. syringae* that do not produce fluorescent siderophores in order to understand how these strains fit iron-limiting conditions. Using conditions known to favor siderophore production (7), we identified a new siderophore which is produced by all nonfluorescent strains of *P. syringae* pv. aptata investigated (Table 1). The production of this siderophore is iron regulated (Fig. 2) in a way similar to that reported for the fluorescent siderophore of *P. syringae* (9). However, we did not detect siderophore production by nonfluorescent strains belonging to other pathovars of *P. syringae* (Table 1). The way these strains fit iron-limiting conditions remains thus unclear.

The molecular mass of the Fe(III) chelate obtained from the fluorescent siderophore produced by *P. syringae* is 1,175 amu. Given the amino acid composition of the molecule, this mass is in total accordance with the predicted value calculated for a pyoverdin that would contain a cyclized peptide chain and a succinamide residue. In addition, the detection of the RDA fragment ion of *m/z* 819 (loss of 302 mass units) in the FAB analyses is diagnostic of a pyoverdin containing a succinamide residue (1, 11, 16, 22). Finally, the spectral characteristics of the unchelated molecule, and the color and spectral characteristics of the Fe(III)-chelated molecule near pH 3.0 (Fig. 3A), resemble those of typical pyoverdins (2, 11, 27). These observations strongly suggest that the molecule is a pyoverdin. However, all Fe(III)-chelated pyoverdins described so far have pH-independent color and spectral characteristics between pH 3.0 and 8.0 (2), but the molecule produced by *P. syringae* does not (Fig. 3A and 4A). The differences are related to the chelation of iron. There is only one difference that could account for the unique behavior of the Fe(III)-chelated pyoverdin produced by *P. syringae*: the unique presence of two β-OH-Asp and no N^{δ}-acyl-N^{δ}-OH-Orn or N^{δ}-OH-Orn involved in the chelation of iron (Fig. 1A) (7, 9). The spectral characteristics of the molecule change in the zone of pH of pK_a of carboxylic acids in a way indicating a unique modification (Fig. 4A). Besides, the iron-binding site of the β-OH-Asp residues contains two hydroxy groups, a β-hydroxy group and a γ-carboxylic acid group (Fig. 1A), but only one group loses a hydrogen to chelate the iron. Therefore, one possible explanation is that the ionization occurring around pH 4.5 of one or two γ-carboxylic acids from the β-OH-Asp residues modifies the way iron is ligated to these β-OH-Asp residues and to the iron-binding site of the chromophore at higher pH. Such a reversible modification would explain the observed reversible changes in the color and spectral characteristics of the molecule. The spectral differences in the visible at neutral pH between the chelated pyoverdin of *P. syringae* and typical pyoverdins produced by saprophytic and opportunistic animal pathogen fluorescent *Pseudomonas* species indicate that the iron should not be similarly bound to the chromophore of these molecules. The differences could explain the higher Fe(III)-binding constants of the pyoverdin of *P. syringae* in neutral and alkaline conditions compared to pyoverdins containing only N^{δ}-acyl-N^{δ}-OH-Orn and N^{δ}-OH-Orn (9, 27). This could have ecological importance since these conditions are favorable to the growth of fluorescent pseudomonads.

Dihydropyoverdins are two mass units higher than the cognate pyoverdins in which they convert by a base-catalyzed air oxidation (38). The same observations were made in this study

with the nonfluorescent siderophore and the cognate fluorescent molecule (Fig. 5). In addition, the color and spectral characteristics of the molecule and of its Fe(III) chelate below pH 4.5 (Fig. 3B and 4B) are close to those reported for dihydropyoverdins (2, 16, 37). However, the spectral characteristics of the Fe(III) chelate change abruptly between pH 3.5 and 5.5 (Fig. 4B), and the molecule is pinkish mauve with an absorbance maximum near 490 nm at neutral pH, rather than reddish-violet with a maximum near 530 to 540 nm, as reported for dihydropyoverdins (2, 16, 37). These results strongly suggest that the nonfluorescent siderophore is a dihydropyoverdin, but that the presence of two β-OH-Asp residues influences the spectral characteristics of the Fe(III) chelate. This is the first report showing that dihydropyoverdins can be the dominant siderophore produced by fluorescent pseudomonads, rather than a by-product that accompanies the production of the cognate pyoverdin (2, 16, 35, 37). However, it cannot be ruled out that some fluorescent *P. syringae* strains could produce the dihydropyoverdin in low quantity. The similarities of the fluorescent and nonfluorescent siderophores explain the similar results obtained in the biological tests with both molecules (7) since the ability to use a pyoverdin or a dihydropyoverdin depends on the peptide chain (38). Whether it is ecologically profitable, or adequate, for the nonfluorescent strains of *P. syringae* pv. aptata isolated from sugar beet to produce a siderophore with a lower Fe(III)-binding constant remains unclear. Also, it is unknown if these strains can be encountered on other hosts of pathovar aptata, such as wheat, bean, and cantaloupe (14, 26, 31).

Strains belonging to the saprophytic fluorescent *Pseudomonas* group, which includes all saprophytic and opportunistic animal pathogen species, are encountered on plants and produce pyoverdins. Therefore, criteria other than fluorescence are needed to classify a fluorescent pseudomonad isolated from plants in the phytopathogenic fluorescent *Pseudomonas* group. The visual, spectrophotochemical (Fig. 6) and electrophoretical (Fig. 7 and 8) pyoverdin detection tests described in this study, however, enable direct distinction to be made between saprophytic fluorescent *Pseudomonas* species and fluorescent strains of *P. syringae* and *P. viridiflava*. Some of these tests are very simple and could be used as confirmation tests in many practical situations when a typical symptom is observed on a diseased plant. However, the tests do not directly indicate the virulence of a strain since pyoverdin production is not essential for the virulence of *P. syringae* (10). The dihydropyoverdin has appeared until now to be specific to nonfluorescent strains of *P. syringae* pv. aptata (Table 1). Unlike the fluorescent strains of the pathovar, the nonfluorescent strains do not use myoinositol (26), but they also produce toxic lipodepsipeptides (6, 26), and the relatedness of all of these strains is now confirmed by the similarities of their siderophores. However, no similarity can be found with the typical pyoverdin produced by two strains isolated from sugar beet in Germany, which contain totally different peptide chains, one N^{δ}-acyl-N^{δ}-OH-Orn and one N^{δ}-OH-Orn (5, 35). These two strains were named *Pseudomonas aptata* 4a and 4b (5, 35), but this nomenspecies is no longer used (12, 33); the name *P. syringae* pv. aptata should have been used. This is surprising given the great differences between the molecules and the general production of an atypical pyoverdin by *P. syringae* (Table 1) and by strains of *P. syringae* pv. aptata, including a German strain, that have been well characterized with regard to their physiology and their virulence in a previous study (26). Moreover, *P. syringae* pv. aptata is not an outlier in *P. syringae* since its pathotype strain is genetically and phenotypically very close to the type strain of *P. syringae*: *P. syringae* pv. syringae LMG 1247 (NCPPB 281, ATCC 19310) (25, 33). Therefore, it seems that further investigations are necessary before a conclusion can be reached on the classification of the two variant German isolates. Also, the partial characteristics reported for a more closely related peptide siderophore produced by one strain of an undetermined pathovar of *P. syringae* (40) are inconsistent with both the characteristics of typical pyoverdins and those of the dominant pyoverdin of *P. syringae*. However, analyses in progress involving more than 200 *P. syringae* strains distributed in more than 30 pathovars indicate that such strains are apparently marginal (unpublished results). The siderophore detection tests described in this study could be used for classification and identification purposes as proposed for *P. aeruginosa* (28). We propose to classify the strains of *P. syringae* pv. aptata as siderovar 1 if they produce the fluorescent atypical pyoverdin, siderovar 2 if they produce the nonfluorescent atypical dihydropyoverdin, and siderovar 3 if they produce the typical pyoverdin. The siderophore-based tests could thus enable the direct identification of pathogenic strains isolated from sugar beet as *P. syringae* pv. aptata siderovar 2.

ACKNOWLEDGMENTS

We thank B. Wathelet for amino acid analyses and R. Rozenberg for expert handling of the mass spectrometers. We are grateful to B. de Ryckel for use of the Shimadzu spectrophotometer.

The work was supported by the Ministère des Classes Moyennes et de l'Agriculture de Belgique, and, for the mass spectrometry part, by the Belgian National Fund for Scientific Research (FNRS).

REFERENCES

1. **Budzikiewicz, H.** 1991. Peptide siderophores from bacteria, p. 537–557. *In* Atta-ur-Rhaman (ed.), Studies in natural products chemistry, vol. 9. Elsevier, Amsterdam, The Netherlands.
2. **Budzikiewicz, H.** 1993. Secondary metabolites from fluorescent pseudomonads. FEMS Microbiol. Rev. **104:**209–228.
3. **Budzikiewicz, H.** 1994. The biosynthesis of pyoverdins. Pure Appl. Chem. **66:**2207–2210.
4. **Budzikiewicz, H.** 1997. Siderophores of fluorescent pseudomonads. Z. Naturforsch. **52c:**713–720.
5. **Budzikiewicz, H., H. Schröder, and K. Taraz.** 1992. Zur Biogenese der *Pseudomonas*-Siderophore: der Nachweis analoger Strukturen eines Pyoverdin-Desferribactin-Paares. Z. Naturforsch. **47c:**26–32.
6. **Bultreys, A., and I. Gheysen.** 1999. Biological and molecular detection of toxic lipodepsipeptide-producing *Pseudomonas syringae* strains and PCR identification in plants. Appl. Environ. Microbiol. **65:**1904–1909.
7. **Bultreys, A., and I. Gheysen.** 2000. Production and comparison of peptide siderophores from strains of distantly related pathovars of *Pseudomonas syringae* and *Pseudomonas viridiflava* LMG 2352. Appl. Environ. Microbiol. **66:**325–331.
8. **Buyer, J. S., and J. Leong.** 1986. Iron transport-mediated antagonism between plant growth-promoting and plant-deleterious *Pseudomonas* strains. J. Biol. Chem. **261:**791–794.
9. **Cody, Y. S., and D. C. Gross.** 1987. Characterization of pyoverdin$_{pss}$, the fluorescent siderophore produced by *Pseudomonas syringae* pv. *syringae*. Appl. Environ. Microbiol. **53:**928–934.
10. **Cody, Y. S., and D. C. Gross.** 1987. Outer membrane protein mediating iron uptake via pyoverdin$_{pss}$, the fluorescent siderophore produced by *Pseudomonas syringae* pv. *syringae*. J. Bacteriol. **169:**2207–2214.
11. **Demange, P., A. Bateman, C. Mertz, A. Dell, Y. Piemont, and M. A. Abdallah.** 1990. Bacterial siderophores: structures of pyoverdins Pt, siderophores of *Pseudomonas tolaasii* NCPPB 2192, and pyoverdins Pf, siderophores of *Pseudomonas fluorescens* CCM 2798. Identification of an unusual natural amino acid. Biochemistry **29:**11041–11051.
12. **Dye, D. W., J. F. Bradbury, M. Goto, A. C. Hayward, R. A. Lelliot, and M. N.**

Schroth. 1980. International standards for naming pathovars of phytopathogenic bacteria and a list of pathovar names and pathotype strains. Rev. Plant Pathol. **59:**153–168.
13. **Garrett, C. M. E., C. G. Panagopoulos, and J. E. Crosse.** 1966. Comparison of plant pathogenic pseudomonads from fruit trees. J. Appl. Bacteriol. **29:** 342–356.
14. **Gross, D. C., and J. E. De Vay.** 1977. Population dynamics and pathogenesis of *Pseudomonas syringae* in maize and cowpea in relation to the in vitro production of syringomycin. Phytopathology **67:**475–483.
15. **Gross, D. C., Y. S. Cody, E. L. Proebsting, Jr., G. K. Radamaker, and R. A. Spotts.** 1983. Distribution, population dynamics, and characteristics of ice nucleation-active bacteria in deciduous fruit tree orchards. Appl. Environ. Microbiol. **46:**1370–1379.
16. **Gwose, I., and K. Taraz.** 1992. Pyoverdins aus *Pseudomonas putida*. Z. Naturforsch. **47c:**487–502.
17. **Hartwig, R. C., and R. H. Loeppert.** 1993. Evaluation of soil iron, p. 465–482. *In* L. L. Barton and B. C. Hemming (ed.), Iron chelation in plants and soil microorganisms. Academic Press, San Diego, Calif.
18. **Höfte, M.** 1993. Classes of microbial siderophores, p. 3–26. *In* L. L. Barton and B. C. Hemming (ed.), Iron chelation in plants and soil microorganisms. Academic Press, San Diego, Calif.
19. **King, E. O., M. K. Ward, and D. E. Raney.** 1954. Two simple media for the demonstration of pyocyanin and fluorescein. J. Lab. Clin. Med. **44:**301–307.
20. **Koedam, N., E. Wittouck, A. Gaballa, A. Gillis, M. Höfte, and P. Cornelis.** 1994. Detection and differentiation of microbial siderophores by isoelectric focusing and chrome azurol S overlay. BioMetals **7:**287–291.
21. **Lindow, S. E., D. C. Arny, and C. D. Upper.** 1978. Distribution of ice-nucleation-active bacteria on plants in nature. Appl. Environ. Microbiol. **36:**831–838.
22. **Linget, C., P. Azadi, J. K. MacLeod, A. Dell, and M. A. Abdallah.** 1992. Bacterial siderophores: the structures of the pyoverdins of *Pseudomonas fluorescens* ATCC 13525. Tetrahedron Lett. **33:**1737–1740.
23. **Loper, J. E., and S. E. Lindow.** 1994. A biological sensor for iron available to bacteria in their habitats on plant surfaces. Appl. Environ. Microbiol. **60:** 1934–1941.
24. **Loper, J. E., and M. D. Henkels.** 1997. Availability of iron to *Pseudomonas fluorescens* in rhizosphere and bulk soil evaluated with an ice nucleation reporter gene. Appl. Environ. Microbiol. **63:**99–105.
25. **Manceau, C., and A. Horvais.** 1997. Assessment of genetic diversity among strains of *Pseudomonas syringae* by PCR-restriction fragment length polymorphism analysis of rRNA operons with special emphasis on *P. syringae* pv. tomato. Appl. Environ. Microbiol. **63:**498–505.
26. **Maraite, H., and J. Weyns.** 1997. *Pseudomonas syringae* pv. aptata and pv. atrofaciens, specific pathovars or members of pv. syringae, p. 515–520. *In* K. Rudolph, T. J. Burr, J. W. Mansfield, D. Stead, A. Vivian, and J. Von Kietzell (ed.), *Pseudomonas syringae* pathovars and related pathogens. Kluwer Academic Publishers, London, England.
27. **Meyer, J. M., and M. A. Abdallah.** 1978. The fluorescent pigment of *Pseudomonas fluorescens*: biosynthesis, purification and physiological properties. J. Gen. Microbiol. **107:**319–328.
28. **Meyer, J. M., A. Stintzi, D. De Vos, P. Cornelis, R. Tappe, K. Taraz, and H. Budzikiewicz.** 1997. Use of siderophores to type pseudomonads, the three *Pseudomonas aeruginosa* pyoverdin systems. Microbiology **143:**35–43.
29. **Michels, J., and K. Taraz.** 1991. Characterization of pyoverdins and their hydrolytic degradation products by fast atom bombardment and tandem mass spectrometry. Org. Mass Spectrom. **26:**899–902.
30. **Morgan. J. V., and H. B. Tukey, Jr.** 1964. Characterisation of leachate from plant foliage. Plant Physiol. **39:**590–593.
31. **Morris, C. E., C. Glaux, X. Latour, L. Gardan, R. Samson, and M. Pitrat.** 2000. The relationship of host range, physiology, and genotype to virulence on cantaloupe in *Pseudomonas syringae* from cantaloupe blight epidemics in France. Phytopathology **90:**636–646.
32. **Page, W. J.** Growth conditions for the demonstration of siderophores and iron-repressible outer membranes proteins in soil bacteria, with an emphasis on free-living diazotrophs, p. 75–110. *In* L. L. Barton and B. C. Hemming (ed.), Iron chelation in plants and soil microorganisms. Academic Press, San Diego, Calif.
33. **Palleroni, N. J.** 1984. Family I. *Pseudomonadaceae*, p. 141–199. *In* N. R. Krieg and J. G. Holt (ed.), Bergey's manual of determinative bacteriology. William & Wilkins Co., Baltimore, Md.
34. **Raaijmakers, J. M., L. van der Sluis, M. Koster, P. A. H. M. Bakker, P. J. Weisbeek, and B. Schippers.** 1994. Utilization of heterologous siderophores and rhizosphere competence of fluorescent *Pseudomonas* spp. Can. J. Microbiol. **41:**126–135.
35. **Schröder, H., J. Adam, K. Taraz, and H. Budzikiewicz.** 1995. Dihydropyoverdinsulfonsäuren-Zwischenstufen beider Biogenese. Z. Naturforsch. **50c:**616–621.
36. **Schwyn, B., and J. B. Neilands.** 1987. Universal chemical assay for the detection and determination of siderophores. Anal. Biochem. **160:**47–56.
37. **Taraz, K., D. Seinsche, and H. Budzikiewicz.** 1991. Pseudobactin-und Pseudobactin A-Varianten: Neue Peptidsiderophore vom Pyoverdin-Typ aus *Pseudomonas fluorescens "E2."* Z. Naturforsch. **46c:**522–526.
38. **Teintze, M., and J. Leong.** 1981. Structure of pseudobactin A, a second siderophore from plant growth promoting *Pseudomonas* B10. Biochemistry **20:**6457–6462.
39. **Teintze, M., M. B. Hossain, C. L. Barnes, J. Leong, and D. van der Helm.** 1981. Structure of ferric pseudobactin, a siderophore from plant growth promoting *Pseudomonas*. Biochemistry **20:**6446–6457.
40. **Torres, L., J. E. Perez-Ortin, V. Tordera, and J. P. Beltran.** 1986. Isolation and characterization of an Fe(III)-chelating compound produced by *Pseudomonas syringae*. Appl. Environ. Microbiol. **52:**157–160.
41. **Wendenbaum, S., P. Demange, A. Dell, J. M. Meyer, and M. A. Abdallah.** 1983. The structure of pyoverdine *Pa*, the siderophore of *Pseudomonas aeruginosa*. Tetrahedron Lett. **24:**4877–4880.
42. **Wilson, M., and S. E. Lindow.** 1994. Coexistence among epiphytic bacterial populations mediated through nutritional resource partitioning. Appl. Environ. Microbiol. **60:**4468–4477.
43. **Wilson, M., and S. E. Lindow.** 1994. Ecological similarity and coexistence of epiphytic ice-nucleating (ice^+) *Pseudomonas syringae* strains and a non-ice-nucleating (ice^-) biological control agent. Appl. Environ. Microbiol. **60:** 3128–3137.